

# Analysis of the Performance a PV System Based on Empirical Data in a Real World Context

Seyed Amin Tabatabaei and Jan Treur

**Abstract** The performance of solar energy production systems consisting of photovoltaic solar panels strongly depends on the location and orientation of the solar panels. Previously a computational model has been developed to predict this performance depending on location and orientation; this model allows for prior analysis of a PV system before it is actually built. In the current paper the performance of solar panels according to their location and orientation is analyzed based on empirical real world performance data, and compared to the data generated by the previously developed computational model. These empirical data have been collected from a number of solar panels at different locations and orientations day-by-day and panel-by-panel for a whole year. The data is analyzed and used to deepen the prior analysis, and to evaluate the computational model thereby generating suggestions for improvement of this model. These suggestions are a basis for an improved computational model in order to enhance the quality of prior analysis of a PV system before it is actually built. Such a pre-analysis is useful as a support for decision making by estimating how much loss different options for locations will have, before actually placing the solar panels.

## 1 Introduction

In recent years, the production of solar energy by photovoltaic panels has increased substantially, which goes hand in hand with strongly decreasing costs of solar panels over the years; e.g., [1–3]. To consider a site for a solar energy plants the

---

S.A. Tabatabaei (✉) · J. Treur  
Agent Systems Research Group, Department of Computer Science, VU University  
Amsterdam, De Boelelaan 1081, 1081HV Amsterdam, The Netherlands  
e-mail: s.tabatabaei@vu.nl

J. Treur  
e-mail: j.treur@vu.nl  
URL: <http://www.cs.vu.nl/~treur>

© Springer International Publishing Switzerland 2015  
A.Y. Oral et al. (eds.), *2nd International Congress on Energy Efficiency  
and Energy Related Materials (ENEFM2014)*, Springer Proceedings in Energy,  
DOI 10.1007/978-3-319-16901-9\_52

circumstances of the site play an important role. For example, how much shadow occurs over the year, is a perfect southward position possible, and is optimal vertical angle of the panels possible? And if not, how much loss is implied by the imperfections of the site? These are not trivial issues to address. For example, if shadow occurs, the extent of the entailed loss in production depends on the specific day in the year and hour of the day. All these have to be aggregated to obtain how much loss this entails over a year. In [4] this has been addressed by an (agent-based) computational model, allowing performing simulations over a whole year. Such a model is very useful for a prior analysis of a site and the different locations within the site, as a basis for decisions on which locations within the site to use. However, the validity of such a computational model has to be assessed based on empirical data. This was not yet done in [4], but is the focus of the current paper.

In the current paper, the performance of solar panels according to their location and orientation is analyzed based on empirical real world performance data. Moreover, the empirical results are compared to the data generated by the computational model described in [4]. The empirical data have been collected at the same site addressed in [4] from a number of solar panels at different locations and orientations day-by-day and panel-by-panel for a whole year. The data is analyzed and used on the one hand to deepen the prior analysis, and on the other hand to evaluate the computational model. This will also provide suggestions for improvement of the computational model. These suggestions are useful as a basis for an improved computational model in order to enhance the quality of prior analysis of a PV system before it is actually built.

In the paper, in Sect. 2 a brief description of the computational model is given; for a more extensive description, see [4]. Section 3 discusses the empirical data, and in Sect. 4 these data are compared to data predicted by the computational model. In Sect. 5 suggestions are discussed for improvements of the computational model.

## 2 The Computational Model

The computational model introduced in [4] describes how at any point in time, the efficiency of the production of a panel depends on situational circumstances. In general, the energy production can be described at each point in time as a function of:

- the available irradiation  $irr$
- the efficiency factor  $\rho_a$  due to angle and orientation of the panel
- the efficiency factor  $\rho_s$  due to shadow
- the efficiency factor  $\rho_{panel}$  of the panel
- the efficiency factor  $\rho_{inv}$  of the micro-inverter

Here it is assumed that the inverter has a peak power that is high enough to process all power provided by the panel. The following relations are assumed:

$$P_{panel} = \rho_a \rho_s \rho_{panel} irr$$

$$P_{out} = \rho_{inv} P_{panel} = \rho_{inv} \rho_a \rho_s \rho_{panel} irr$$

where  $P_{panel}$  is the power provided by panel and  $P_{out}$  by the inverter. Note that  $\rho_{panel}$  and  $\rho_{inv}$  are given characteristics of the panel and inverter, and  $\rho_s$ ,  $\rho_a$ , and  $irr$  are situational variables that can be manipulated or depend on time of the day and year. In an ideal situation, it holds  $\rho_s = \rho_a = 1$  (no shadow and most optimal angles). For input on irradiation for different times in a year, realistic empirical data were acquired (from the Dutch Meteorological Institute KNMI). Note that such information for Europe can also be obtained at [5].

Moreover, note that to compare the situational aspects for two different options for locations (1) and (2) at the same site (when it is assumed that  $\rho_{inv}(2) = \rho_{inv}(1)$ ,  $\rho_{panel}(2) = \rho_{panel}(1)$  and  $irr(2) = irr(1)$ ), by dividing some of the factors can be left out:

$$\frac{P_{panel}(2)}{P_{panel}(1)} = \frac{\rho_{inv}(2)\rho_a(2)\rho_s(2)\rho_{panel}(2) irr(2)}{\rho_{inv}(1)\rho_a(1)\rho_s(1)\rho_{panel}(1) irr(1)} = \frac{\rho_a(2)\rho_s(2)}{\rho_a(1)\rho_s(1)}$$

In particular, when situation (1) is an ideal situation it holds  $\rho_a(1)\rho_s(1) = 1$ , then  $\rho_a(2)\rho_s(2)$  indicates how situation (2) performs in comparison to most optimal. Given this, the loss percentage of a situation in comparison to an ideal situation can be obtained as  $100 * (1 - \rho_a \rho_s)$  or as an approximation  $100 * (1 - \rho_s) + 100 * (1 - \rho_a)$ . For a real world site there may not be such an ideal situation. Then a relative loss percentage can be used, with respect to the most optimal situation within the site.

### 2.1 Modeling Shadow Effects: The Variable $\rho_s$

How shadow affects the energy production (the variable  $\rho_s$ ) directly relates to obstacles on the one hand, and positions of the sun on the other hand. The position of the sun (seen from the earth) is characterized by two angles (see also [6]): the vertical angle above the horizon, and the horizontal angle with the direction of North. These are modeled as a function of time and based on this by geometry for each relevant obstacle the shadow length over time is determined, from which it is found at which time points a given location has shadow.

### 2.2 Modeling the Effects of Panel Orientation and Angle: The Variable $\rho_a$

The orientation and angle under which the panel is positioned is another important factor (the variable  $\rho_a$ ). For example, at [7] a schematic overview is shown of how

efficiency relates to the vertical and horizontal angle of a panel, taken over a year. This is modeled for the South South West orientation of the site as an approximation (with  $\alpha$  the panel angle with the horizontal plane)

$$\rho_\alpha = 0.58 \sin(\alpha + 55) + 0.39$$


### 3 The Real World Situation and the Empirical Data

In this section the considered real world situation and the empirical data that have been collected will be described.

#### 3.1 The Locations and the Data Collection



The considered real world situation fulfills the requirement that it consists of locations that are not ideal. Overall, the real world situation concerns a three storey family house (a net-zero house using a heat pump for heating) in an environment with many high trees, near Alkmaar, the Netherlands (about 52.6 latitude, 4.7 longitude). More specifically, all of the considered locations suffer from periods with shadow, and most of the locations do not allow for panel positions with an ideal vertical angle. Furthermore, the orientation of the whole site is not South but South West. All these dimensions of imperfectness, inherent to real life and real world sites, provide good possibilities to investigate in a comparative manner how they affect the production over a year. Four possible locations for solar panels have been used, as briefly described below (Table 1). Note that location 2 has been left out of consideration here because no adequate data for a full year were available for it (due to a change of positions within the year).

**Table 1** Possible locations for solar panels

<p><i>Location 1 (6 panels)</i> Shelter in the garden with an almost flat roof oriented South South West with shadow from the house with height 5.00 m at a distance of 6.00–10.00 m South East and from various trees. Vertical panel angle is 15°</p>	
<p><i>Location 3 (8 panels)</i> Flat roof at top of a dormer oriented South South West with shadow from a row of trees East South East at a distance of 8.50–15.50 m and height 5.50 m above the</p>	

(continued)

**Table 1** (continued)

<p>roof and from the rooftop South South West at a distance of 0.85–3.00 m with height 0.50 m. Vertical panel angles are 1° and 10°</p>	
<p><i>Location 4 (7 panels)</i> Sloped roof oriented South South West with shadow from a row of trees East South East at a distance of 8.50–15.50 m and height 5.50 m above the roof. Vertical panel angle is 30°</p>	

The panels used are Renesola [8] 265 Wp monocrystalline panels. Moreover, Power One [9] 300 W micro-inverters are used, allowing to monitor each panel separately through the Aurora CDD central monitoring device which communicates radio graphically with all micro-inverters and through Wi-Fi with a computer.

For these locations every day data were collected for the day production for every panel. This has been done from the beginning of June 2013 and is still continuing during fall 2014. In the current paper the data are used for exactly 1 year: from the beginning of June 2013 to the end of May 2014.

### 3.2 Initial Analysis of the Empirical Data

In this section the available data are briefly reviewed. In Sect. 4 the analysis goes further and focuses on comparison with the predicted data. First, in Fig. 1 the year production is shown for each panel. Indeed the different locations show different yields, with location 4 as the best. Also within the locations differences are shown. For example, a clear trend is visible that the panels more close to the row of trees have lower production. In the graph, two lines have been added that indicate the levels predicted by a rule of thumb often used in the Netherlands. This rule of thumb (in principle meant for ideal locations) says that a PV system of p Wp will provide a year production of 0.85 p kWh, i.e., kWh/Wp = 0.85 (conservative variant, red line), or 0.9 p kWh, i.e. kWh/Wp = 0.9 (more optimistic variant, green line). As can be seen location 4 provides more than this, but most other locations less.

It turns out that the first panel of location 4 has the maximum output. Therefore, this panel is used as a norm, and loss percentages have been determined in comparison to this panel. This is shown in Fig. 2 below: loss percentages compared to loc4-1.

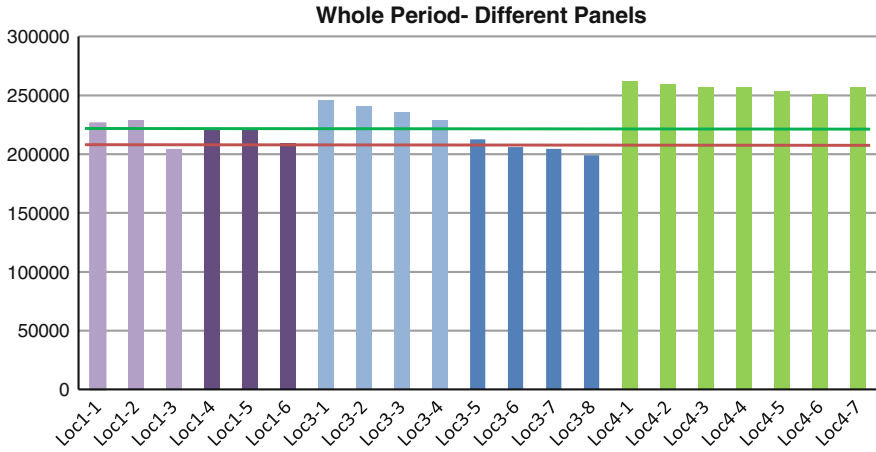


Fig. 1 Empirical data: production of each panel in the 12 months period June 2013–May 2014

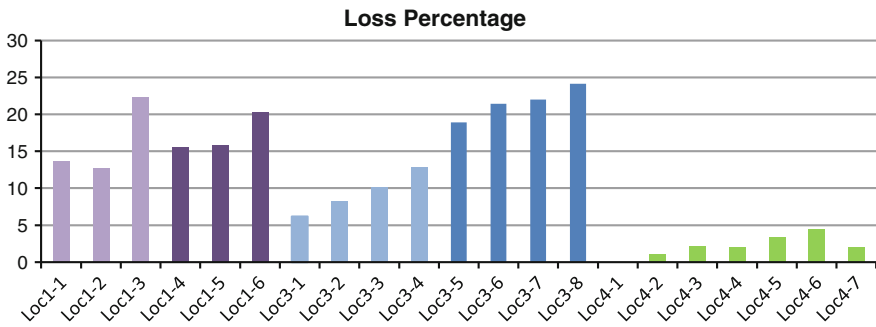


Fig. 2 Loss percentage of each panel in the period of 12 months (June 2013–May 2014)

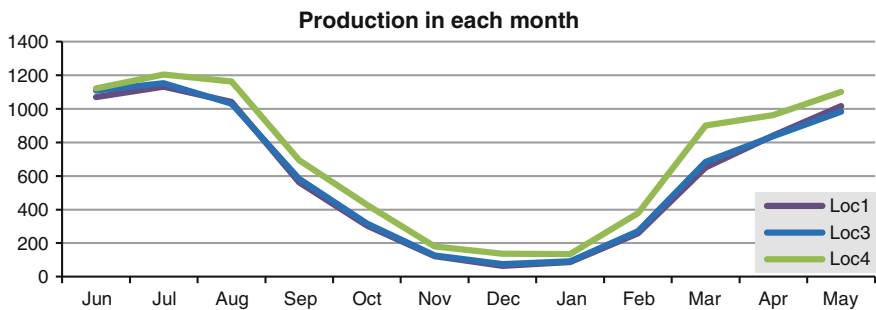


Fig. 3 Empirical data: average production of panels of each group in different months

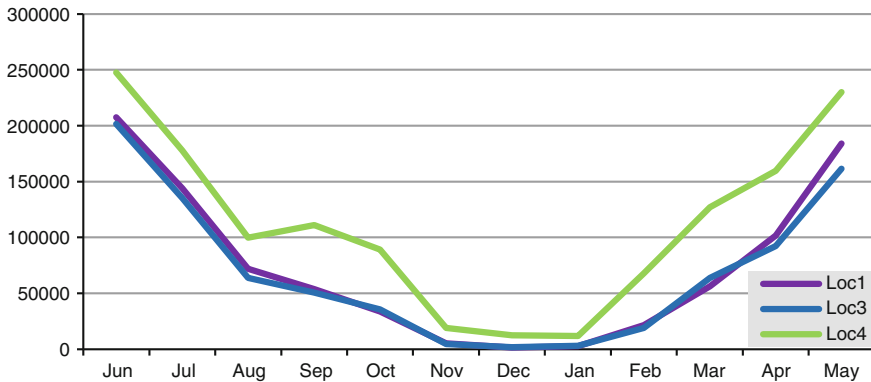


Fig. 4 Empirical data: variance of average of daily production

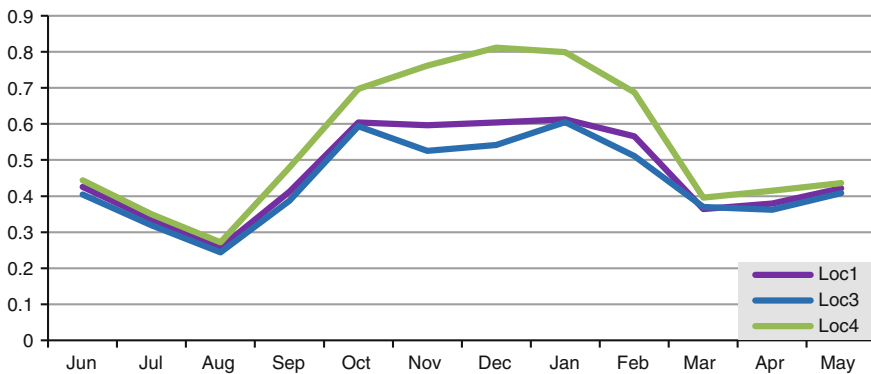
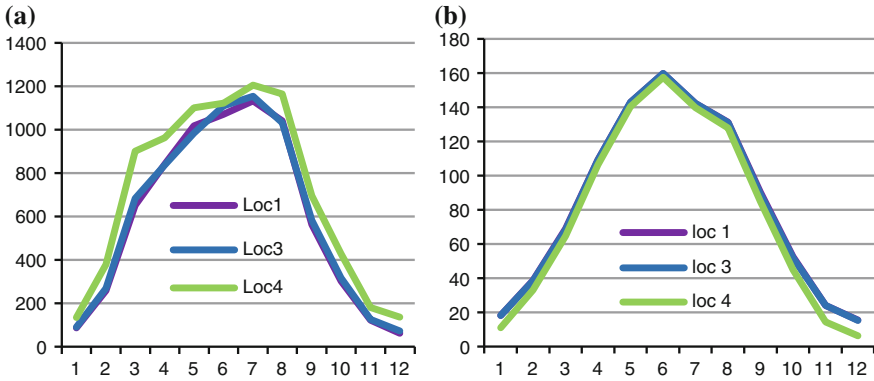


Fig. 5 Empirical data: coefficient of variance of average of daily production in each month

It is shown that within location 4 there is also some loss compared to the norm panel up to 4 %. The other locations show a higher loss percentage. For location 1 the loss goes from 6 to 25 %. Location 3 shows losses from 18 to 24 %.

In Fig. 3 the production of the three locations over the months is shown. It turns out that location 1 and 3 have practically equal production every month and location 4 has a substantially higher production every month.

The production per day shows much variation, especially when the average production per day is high, for example in the months April to August. This is shown in Fig. 4 below. If this is considered relative by dividing the variance by the average, this relative variation (coefficient of variance) is higher in the months October to February (see Fig. 5).



**Fig. 6** **a** Monthly production: empirical data. **b** shadow effects predicted in previous paper

$$C_v = \frac{\text{standard deviation}(\sigma)}{\text{mean}(\mu)}$$

### 4 Comparative Analysis

In this section some of empirical data are compared to the predicted data obtained by the computational model. In Fig. 6a, the same data are depicted as in Fig. 3, but re-ordered from January to December. In this form they can be easily compared to a similar graph for the corresponding predicted data for ideal angles shown in Fig. 6b. In both figures it is clear that the production of location 1 and location 3 is equal for every month, so in that sense the empirical data confirm the predicted data. However, for location 4 in the empirical data a difference is shown with the other two locations, whereas there is almost no such difference in the predicted data in Fig. 6b. This can be easily explained, as for the predictions ideal angles were assumed, whereas in the real world case for location 4 the ideal angle of 30° occurs, but for locations 1 and 3 the angle is less ideal (more in the range of 5°–15°). Therefore in Fig. 6b the differences in irradiation due to shadow are shown and not differences due to angle, whereas in Fig. 6a the differences both due to shadow and angle are shown. It turns out that differences in production due to shadow concentrate in the months September to March, whereas differences in production due to angle differences occur through the whole year.

Note that only the month June seems to be a slight exception, as then location 3 and location 4 shows the same value. This may be an indication that in June relatively often a cloudy weather type has occurred (compared to the average weather in June over the years). For cloudy weather the diffusion radiation plays a most important role, and panels with higher angles have a disadvantage then, as they get radiation from a smaller part of the sky.



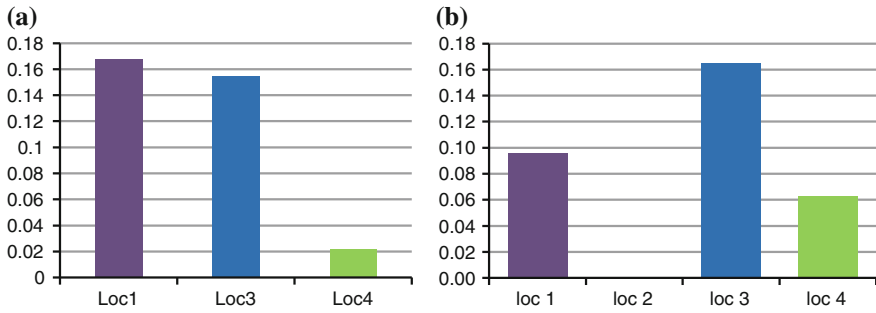


**Fig. 7** Yearly loss percentages **a** empirical data, **b** predictions from previous paper

Moreover, the top in the empirical data is in July whereas the top in the predicted data is in June. This can be explained by the fact that the predicted data is based on average irradiation over the years, whereas in the real world data for only one particular year. Apparently in 2013 the month July provided relatively more irradiation than average, in comparison to June. This is in line with the suggestion above that June may have had more cloudy weather than average.

A check in the meteorological archives from the Dutch Meteorological Institute KNMI for the Netherlands at [10] confirms the explanations suggested above: in June 2013 there were 184 sun hours' versus 201 normally, which indicates 8 % lower than normal. In contrast, for July 2013 it was noted at [11] that there were 255 sun hours' versus normally 212, which is 20 % higher than normal. This indeed confirms the explanations suggested above.

Only when empirical data are collected over 10–20 years averages can be made that can be more similar to the predicted average data. Unfortunately, such empirical data are not available for the considered site.

In Fig. 7a, the loss percentages are shown per location; this is a form of abstraction of the data for loss percentages per panel depicted in Fig. 2. These loss percentages can be compared to the predicted loss percentages (assuming the realistic angles) from [4] shown in Fig. 8b. Note that the graphs are not fully comparable, as in Fig. 8b it shows the losses with respect to an ideal panel, whereas in Fig. 7a losses with respect to a real panel (which by itself is not ideal) are shown. If  $x$  would be the loss percentage of this real panel, then approximately this  $x$  should be added to the values in Fig. 7a. It is not known whether  $x$  is just 1 or 2 % or maybe more, for example 5 %. Suppose this  $x$  is 3 %. Then for location 4 the numbers are almost the same (5 % vs. 6 %), and for location 3 also (18 % vs. 17 %). For these two locations the empirical data seem to confirm the predicted ones. However, for location 1 there is a huge difference (20 % vs. 10 %). In the real world the loss percentage for this location is twice the predicted loss percentage. But there is an explanation for this. In the computational model, to determine the loss due to shadow, the relevant obstacles have to be identified and incorporated. For location 1, only the house as an obstacle was taken into account, as it was the closest

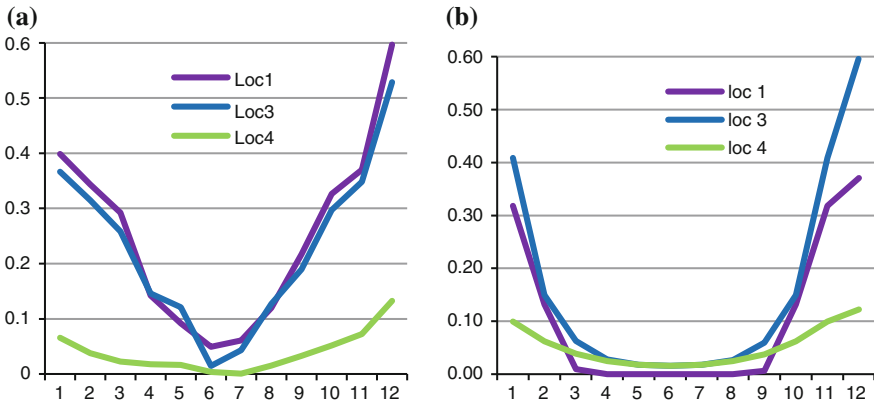


**Fig. 8** Loss percentage in different months **a** empirical data, **b** predictions previous paper

obstacle. However, due to its low position various trees also provide shadow at location 1, both from the row of trees from the front side and from trees in the gardens at the backside. For the sake simplicity, these trees were left out of the calculations, and therefore their effect was just neglected. Now, with the empirical data at hand it may be concluded that this was not a justified modeling decision.

In Fig. 8a the loss percentages are shown for the different locations based on the empirical data. In Fig. 8b the predicted loss percentages are shown for these locations, assuming ideal angles. Again, it becomes clear that the effect of different angles entails differences in loss percentages in Fig. 8a for the months March to September that are not there in Fig. 8b, where the angles are assumed all ideal.

## 5 Discussion and Conclusion

The performance of photovoltaic solar energy production plants (e.g., [1, 2]) can be analyzed prior to their installation based on a computational model, instead of analyzing during their operation based on empirical data (e.g., [12, 13]). Some examples of approaches that can be used for prior analysis based on a simulation model and/or sensitivity analysis are [4, 7, 14].

A plant at a certain site usually is distributed over a number of locations within the site. Often such locations in a site are not always ideal, and may entail loss of efficiency, due to effects of shadow and/or to non-optimal orientations and angles for the panels. The effects of such situational circumstances vary with time of the day and day of the year. Evaluation of performance of an operational plant may be most accurate after at least 1 year, but still the weather circumstances in that year may not be representative for other years. Therefore a prior analysis based on a

computational model is a relevant approach. However, such an approach can benefit much if at least some validation is possible by comparing its results to empirical data.

In this paper the performance of solar panels according to their location and orientation was analyzed based on empirical real world performance data and compared to the data generated by the computational model introduced in [4]. These empirical data have been collected day-by-day and panel-by-panel for 1 year. The data enabled to substantiate the prior analysis. Moreover, they were used to evaluate the computational model, and based on that suggestions for improvement of this model will be discussed here.

The first suggestion for improvement of the computational model concerns the way in which the effects of shadow were modeled. The approach is based on the identification of obstacles one by one and for each of them calculation of the position and length of its shadow at all points in time. It has turned out in Sect. 4 that this is feasible for one or two obstacles. For example, this was the case for location 3 at the considered site, where two obstacles play a role, and the results of the model were not much different from the empirical data. However, when a larger number of obstacles play role, this computational approach easily leads to neglecting some of the obstacles, as each of them requires a lot of work. This was what happened for location 1 of the considered site, and as a result for this location the outcomes from the computational model were about 50 % different from the empirical data. Given this experience, the following suggestion for improvement can be considered. If only one or two obstacles are present, then the current method can be used. But in cases with more obstacles, an alternative method may work with contours of the horizon from a point in the location and compare that to the sun's orbit, such as is advocated, for example, by the Solar Pathfinder [15], or by the method described at [16]. Also this method may require quite a bit of work. Especially as it is point-based, to get accurate results it may have to be applied to different points of a location. But it still may be more feasible than considering a large number of obstacles one by one.

A second suggestion for improvement concerns the role of indirect sunlight due to diffusion. In particular on days with grey or cloudy weather this type of irradiation plays an important role. As discussed in Sect. 4, this may affect production results. For example, panels with an angle of  $0^\circ$  or close to it have an advantage in such circumstances as they are open for receiving irradiation of the whole sky, whereas panels with an angle of, for example,  $35^\circ$  are open for irradiation of only a part of the sky. In the current computational model, such circumstances were not addressed separately. It may be a suggestion to refine the model by handling such type of radiation separately.

The suggestions discussed above can be used as a basis for an improved computational model in order to enhance the quality of prior analysis of a PV system before it is actually built.

## References

1. M.A. Eltawil, Z. Zhao, Grid-connected photovoltaic power systems: technical and potential problems—a review. *Renew. Sustain. Energy Rev.* **14**, 112–129 (2010)
2. B. Parida, S. Iniyar, R. Goic, A review of solar photovoltaic technologies. *Renew. Sustain. Energy Rev.* **15**, 1625–1636 (2011)
3. V.V. Tyagi, N.A. Rahim, J.A. Selvaraj, Progress in solar PV technology: research and achievement. *Renew. Sustain. Energy Rev.* **20**, 443–461 (2013)
4. J. Treur, in *Analysis of configurations for photovoltaic solar energy production using agent-based simulation*, eds. by M. Klusch, M. Thimm, M. Paprzycki. Proceedings of the Second International Workshop on Smart Energy Networks and Multi-Agent Systems, SEN-MAS'13. Lecture Notes in Artificial Intelligence, vol. 8076 (Springer, Verlag, 2013), pp. 372–385
5. URL Irradiation data, <http://re.jrc.ec.europa.eu/pvgis/apps4/pvest.php>
6. C.B. Christensen, G.M. Barker, in *Effects of Tilt and Azimuth on annual incident solar radiation for United States Locations*. Proceedings of Solar Forum 2001—Solar Energy: The Power to Choose. Washington, DC. (2001)
7. H. Ziar, H.K. Karegar, Sensitivity analysis of solar photovoltaic modules to environmental factors through new definitions and formulas. *J. Renew. Sustain Energy* 5.5 (2013)
8. URL Renesola, <http://www.renesola.com>
9. URL Power One Aurora, <http://www.power-one.com/renewable-energy/products/solar/string-inverters/panel-products/aurora-micro/series-0>
10. URL meteorological archives for the Netherlands in June 2013, [http://www.knmi.nl/klimatologie/maand\\_en\\_seizoenoverzichten/maand/jun13.html](http://www.knmi.nl/klimatologie/maand_en_seizoenoverzichten/maand/jun13.html)
11. URL meteorological archives for the Netherlands in July 2013, [http://www.knmi.nl/klimatologie/maand\\_en\\_seizoenoverzichten/maand/jul13.html](http://www.knmi.nl/klimatologie/maand_en_seizoenoverzichten/maand/jul13.html)
12. V. Sharma, S.S. Chandel, Performance analysis of a 190 kWp grid interactive solar photovoltaic power plant in India. *Energy* 1–10 (2013). doi:10.1016/j.energy.2013.03.075
13. L.S. Pantić, T.M. Pavlović, D.D. Milosavljević, A practical field study of performances of solar modules at various positions in Serbia. *Thermal Science* 00 (2014)
14. T. Ma, H. Yang, L. Lu, Solar photovoltaic system modeling and performance prediction. *Renew. Sustain. Energy Rev.* **36**, 304–315 (2014)
15. URL Solar Pathfinder, <http://www.solarpathfinder.com>
16. URL Sun path chart program, <http://solardat.uoregon.edu/SunChartProgram.html>